$T1_\rho$ MRI: A Potential Biomarker of Cartilage Physiology

Arijitt Borthakur, Ph.D.[1]; Walter R. T. Witschey, Ph.D.[1]; Anup Singh, Ph.D.[1]; Hari Hariharan, Ph.D.[1]; Tiejun Zhao, Ph.D.[2]; Niels Oesingmann, Ph.D.[2]; Ravinder Reddy, Ph.D.[1]

[1] *Center for Magnetic Resonance & Optical Imaging, Department of Radiology, Perelman School of Medicine at the University of Pennsylvania, Philapelphia, PA, USA*
[2] *Siemens Medical Solutions, Pittsburgh and Malvern, PA, USA*

Introduction

Osteoarthritis (OA) affects more than half of the population above the age of 65 and has a significant negative impact on the quality of life of elderly individuals. The economic costs in the US from OA have been estimated to be more than 1% of the gross domestic product. Imaging the physiology of cartilage tissue holds promise for an early detection of OA, the most common joint disease whose prevalence will only increase due to an aging population [1]. The disease is characterized by focal cartilage damage, changes in the subchondral bone, mild synovitis, and thickening of the joint capsule in synovial joints. Key to understanding the pathology of the disease is to appreciate that the biochemistry of cartilage tissue underlies its special purposes of control over joint loading and motion. Only a small fraction of the volume of cartilage is occupied by cells (chondrocytes) that facilitate construction, repair and degradation of the extracellular matrix (ECM) in response to stimuli. Water occupies 70% of the volume of the ECM [1] while the major solid constituents (Fig. 1) are aggrecan (5% w/v) and type II collagen (20% w/v).

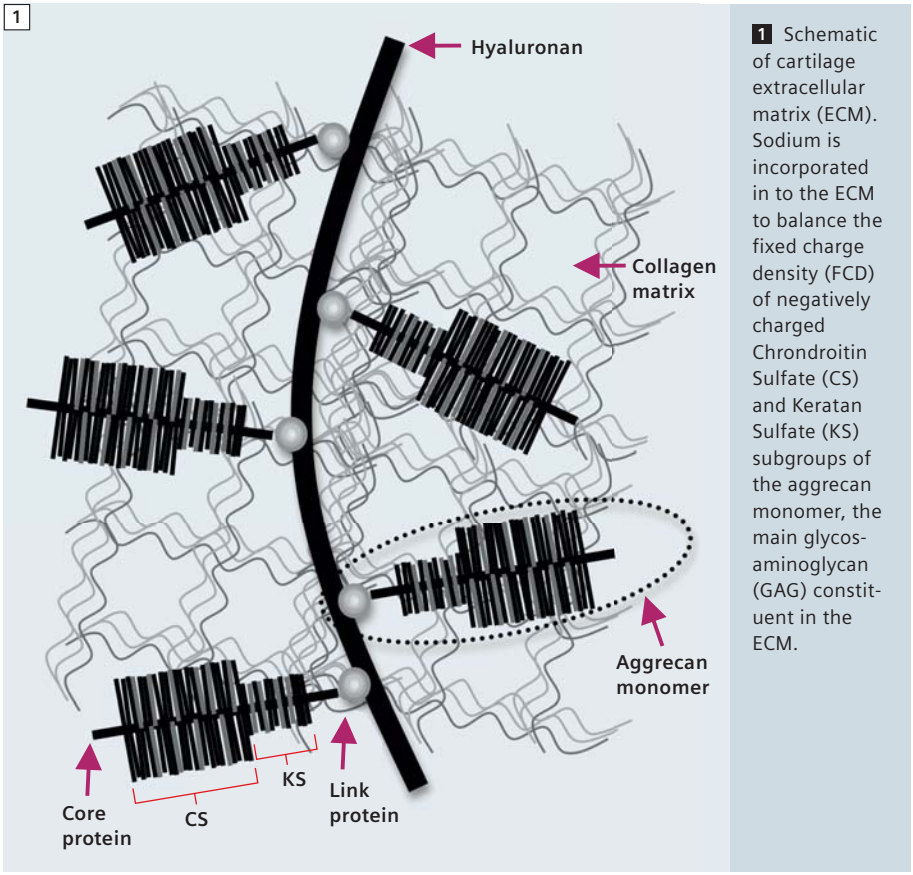

1 Schematic of cartilage extracellular matrix (ECM). Sodium is incorporated in to the ECM to balance the fixed charge density (FCD) of negatively charged Chrondroitin Sulfate (CS) and Keratan Sulfate (KS) subgroups of the aggrecan monomer, the main glycosaminoglycan (GAG) constituent in the ECM.

The early stage of OA is associated with an increase in enzymatic degradation by matrix metalloproteinases resulting in depletion of glycosaminoglycan (GAG) of aggrecan as well as degradation of the collagen network. In cartilage, GAG side chains are made of continuously repeating disaccharides containing carboxyl and sulfate functional groups and are both negatively charged under physiological conditions. The negative charge GAG confers on cartilage is the fixed charge density (FCD). Gorton originally proposed a model for the physiology of connective tissues in which a high polysaccharide content induces an osmotic pressure that is resisted by the network of collagen [2]. In this model, the presence of highly electronegative and immobile GAG macromolecules results in an influx of sodium ions to maintain electro-neutrality. Since then, Maroudas extended this model by introducing the Donnan equilibrium to describe the flux of charged ions across a semi-permeable membrane in the presence of a charged but non-exchanging GAG restricted to a single compartment [3, 4]. In this model, the low hydraulic permeability of GAG counterbalances resistive loads by its swelling pressure while collagen provides tensile and shear strength. Therefore, GAG loss in early OA initiates a cascade by which osmotic pressure is

reduced and joint compression permanently disrupts the cartilage leading to thinning, fracturing and subsequently pain [5, 6].

Current imaging methods for OA

Radiographic imaging is the current gold standard in imaging technology to detect advanced stages of OA. Lacking sensitivity to soft tissues, this X-ray based technique measures joint space narrowing (JSN) to indirectly gauge the extent of damage to cartilage. In addition, outcome instruments for assessment of OA in patients such as the Knee injury and Osteoarthritis Outcome Score (KOOS), an extension of the Western Ontario and McMaster Universities Osteoarthritis Index (WOMAC), is also used to determine mobility and pain in a specific joint [7, 8]. However, radiography, along with nuclear medicine scans, arthrography, and computed tomography (CT) scans, are limited in their use because they are unable to detect early cartilage abnormalities [9]. Conventional T1-weighted and T2w MRI can directly visualize all diarthrodial tissues, including cartilage, bone, synovium, menisci, and ligaments and has substantial advantages over radiography [10–12]. Due to the high morbidity of OA, therapeutic interventions are particularly necessary but current methods are restricted to management of pain and surgical interventions [13]. However, improving outcomes require development of more effective interventions that can slow or reverse the course of the disease. In this context, there is a requirement for strong diagnostic information sensitive to the early stages of the disease, where cartilage appears intact on radiographs. Furthermore, because of the long natural history of OA (10–20 years in humans), sensitive imaging biomarkers are expected to significantly accelerate the drug development process by assessing the therapeutic potential in terms of efficacy at the early stages of the disease and thereby lowering the cost and duration of clinical trials.

The aim of this review is to highlight $T1_\rho$ ($T1\text{-}_{rho}$) MRI, a technique that has been developed to specifically detect the GAG component of cartilage, which is the more important element due to the ostensibly limited contribution of collagen to the initiating steps of OA [14]. Only the salient features of this method are described here with a limited review of the literature.

2

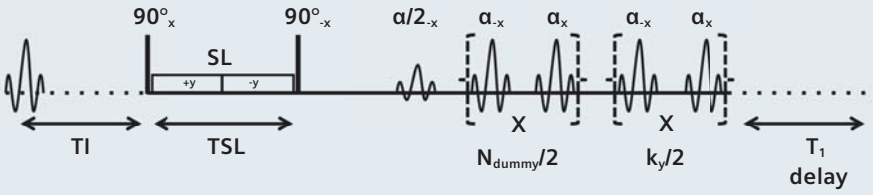

2 Pulse sequence diagram for inversion-prepared $T1_\rho$ MRI with a 3D balanced-GRE readout [38]. TI is the inversion time, TSL is the duration of two phase-alternating spin-lock pulses inserted between two 90° RF pulses, which is followed by a half-α pulse that begins the centric-encoded balanced-GRE readout. A delay time is inserted at the end of the α pulse train for T1 recovery.

3

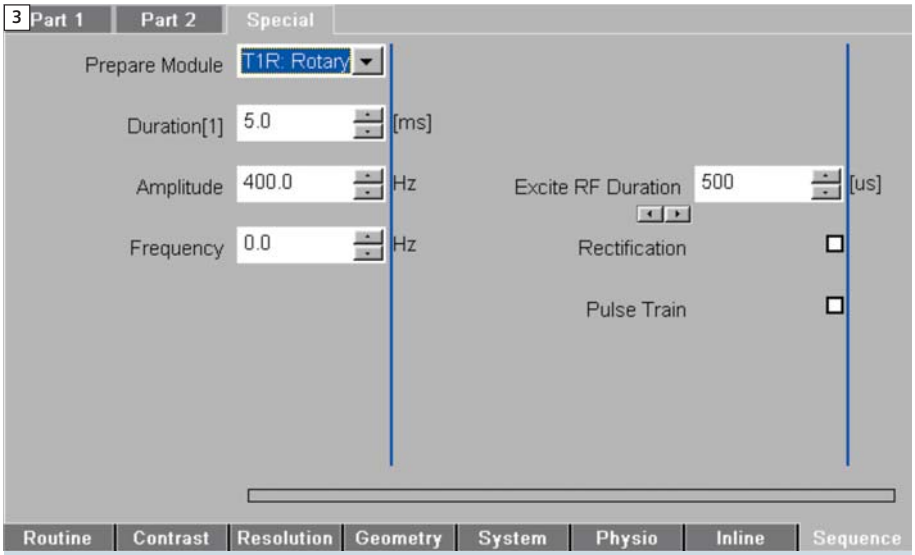

3 The MRI console's Sequence Special tab showing the user controllable variables and typical values associated with the $T1_\rho$ pulse sequence in figure 2. In this particular case, a Rotary Echo $T1_\rho$ preparation is employed with TSL times in multiples of 5 ms. The number of distinct TSL data sets acquired is 5 (entered on Part 2 tab). The γB_1 spin-lock amplitude is set to 400 Hz for a body-coil transmit and 500 Hz for knee-coil transmit. The duration of the 90° hard pulses in the $T1_\rho$ preparation is 500 µs.

$T1_\rho$ MRI

$T1_\rho$ MRI is an alternative to conventional T1w and T2w MRI [15] by its use of a long-duration, low-power radiofrequency (RF) referred to as spin-lock (SL) pulse applied to the magnetization in the transverse plane. The magnetization is effectively spin-locked around an effective B_1 field created by the vector sum of the applied B_1 and any off-resonant component. The spin-locked magnetization will relax with a time constant $T1_\rho$, the spin-lattice relaxation in the rotating frame, during the RF field. The B_1 field attenuates the effect of dipolar relaxation, static dipolar coupling, chemical exchange and background gradients on the signal resulting in a $T1_\rho$ that is always greater than T2. $T1_\rho$ was shown to be influenced by the exchange of hydroxyl (–OH) and amide (–NH) protons on the GAG [16]. There has been consid-

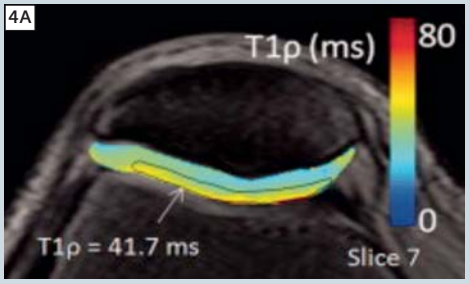

4 **(4A)** $T1_\rho$ relaxation map from a 30-year-old male with no history of knee injury and no knee pain. Patellar cartilage is homogenously, smoothly varying and has a characteristic increase in $T1_\rho$ from the deep cartilage adjacent to the subchondral bone to the superficial cartilage adjacent to the synovium. The ROI drawn at the cartilage surface had a $T1_\rho$ = 41.7 ms.

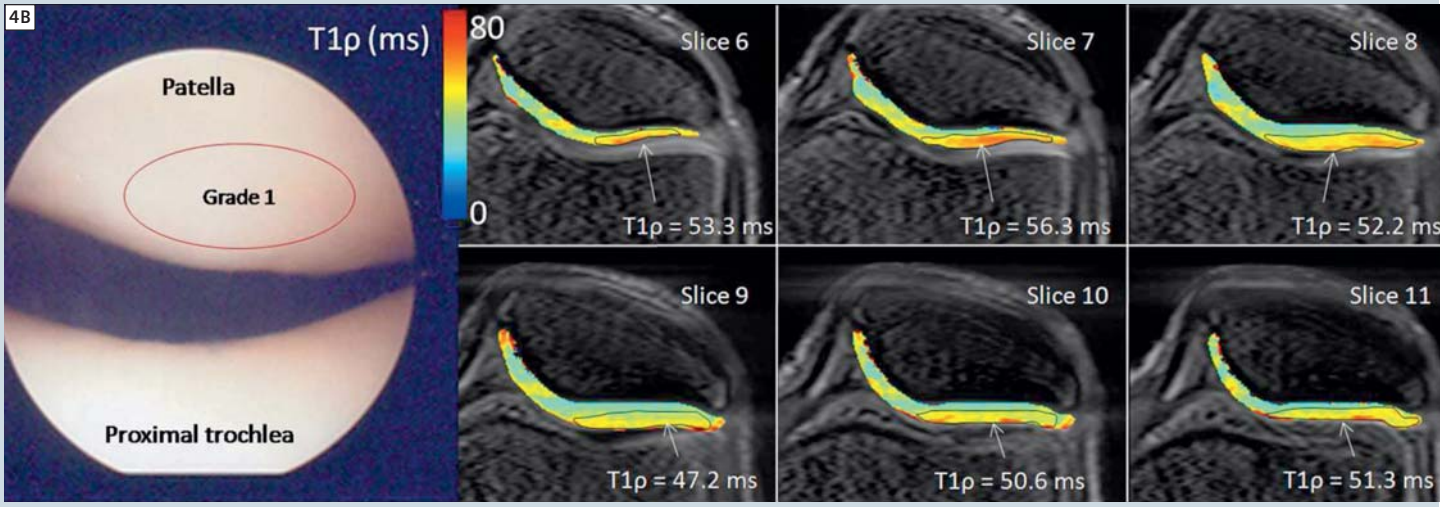

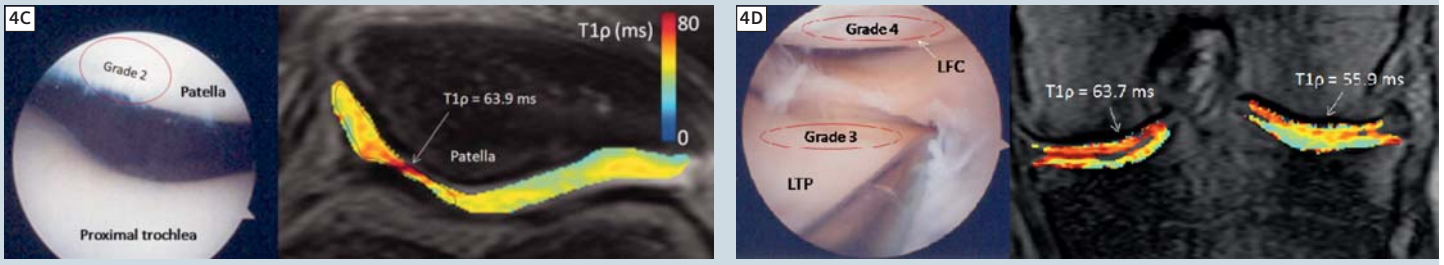

A 76-year-old patient with grade 1 chondromalacia of the lateral patellar facet and grade 2 chondromalacia of the medial patellar facet is shown **(4B)** with elevated focal $T1_\rho$ lesions. Another patient was observed at arthroscopy to have grade 2 patellar chondromalacia and a torn left medial meniscus, for which a partial medial meniscectomy was performed **(4C)**. Similar images are provided to show correspondence between arthroscopic image and $T1_\rho$ maps for grade 3 **(4D)** and grade 4 **(E)** chondromalacia [33].

erable amount of work on biological tissues using $T1_\rho$-spectroscopy and imaging dealing with tumors, muscle, myocardium, blood flow and cartilage [17–27].

Quantitative $T1_\rho$ MRI relaxation relaxometric images can reflect the biochemical composition of cartilage. These $T1_\rho$ 'maps' are created by fitting the signal intensity of $T1_\rho$-weighted MR images as a function of the SL pulse duration with fixed amplitude (γB_1 = 500 Hz). In this manner, spatial maps of $T1_\rho$ values related to macromolecular composition of tissues can be visualized and analyzed. The current protocol for $T1_\rho$ MRI uses a 3D balanced gradient echo readout to detect the $T1_\rho$ prepared magnetization (Fig. 2) that is developed in our lab. Typical user-controllable values for the customer-made pulse sequence are shown in figure 3. This imaging protocol is under 15 minutes for acquiring five $T1_\rho$-weighted 3D data sets for computing color-coded $T1_\rho$ maps showing the spatial distribution of cartilage matrix elements, GAG, water, and collagen. The non-averaged dipolar interaction between water protons associated with collagen is the predominant contributor to relaxation in cartilage [28]. $T1_\rho$-dispersion MRI, where the amplitude of the SL pulse amplitude is also varied, can be used to detect spectral density components in cartilage that are in the neighborhood of γB_1. The effect of spin-locking reduces the laminar appearance in cartilage as demonstrated by Akella et al. in an orientation-dependent MRI experiment of cartilage plugs [29]. In this study, a typical laminar appearance was present in T2 MRI when the normal

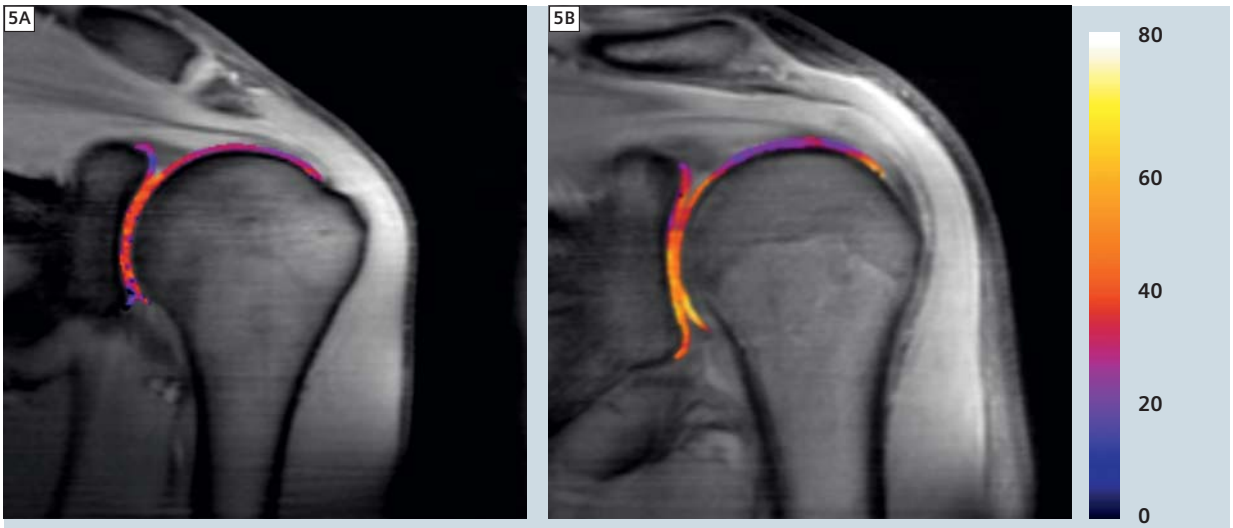

5 Color-coded $T1_\rho$ maps are overlaid on gray scale $T1_\rho$-weighted images for three volunteers: **5A:** 22-year-old healthy, **5B:** 22-year-old volunteer with painful shoulder. Color bar represents $T1_\rho$ values

to the surface of cartilage was parallel to B_0 but absent in $T1_\rho$ MRI of the same cartilage specimen. In addition, $T1_\rho$ values were consistently greater than T2 at all orientations throughout the cartilage layers, a result of spin-locking the magnetization.

$T1_\rho$ in clinical OA research

Several studies have demonstrated the efficacy of $T1_\rho$ MRI in detecting early tissue pathology with increasing values in OA-affected cartilage compared to normal tissue [30]. $T1_\rho$ MRI was also demonstrated to quantitatively evaluate meniscus and cartilage matrix in animal models as well as in patients with acute anterior cruciate ligament (ACL) injuries [31, 32]. Studies on arthroscopically-confirmed early grades of chondromalacia have demonstrated the potential of a rapid MRI pulse sequence (Fig. 4) for $T1_\rho$ mapping in order to detecting earliest molecular changes in cartilage *in vivo* [33].

Another potential application of $T1_\rho$ MRI is in the shoulder joint. Glenohumeral arthritis is a disabling condition, which severely affects the quality of life and activities of recreation and daily living [34]. Primary glenohumeral osteoarthritis predominantly occurs in older individuals; however, a younger cohort of patients has been recently described with end stage glenohumeral arthritis after shoulder arthroscopy [35]. With shoulder injuries, the integrity of the cartilage may become compromised due to several factors such as abnormal loading conditions and repeated stresses. Routine clinical care of shoulder joint is limited to morphologic and structural changes but the sensitivity of $T1_\rho$ to early changes due to arthritis may help in the diagnosis and treatment of the disease. To this end, the $T1_\rho$ mapping technique was applied to normal and shoulder pain subjects on a Siemens clinical 3T scanner with the vendor-supplied shoulder coil. $T1_\rho$ map of the shoulder joint of a healthy volunteer is displayed alongside a patient with shoulder joint pain (Fig. 5). Elevated $T1_\rho$ values in the glenoid compartment cartilage in the latter individual could indicate early cartilage degradation resulting from arthritis. Further research is ongoing on individuals with traumatic shoulder joint injury to quantify early onset of degeneration of cartilage in the joint.

Summary

MRI based on conventional T1 and T2 contrast is able to provide excellent images of cartilage morphology, but could be insensitive to detect changes in cartilage biochemistry and physiology. While OA progression is multi-factorial and slow progressing disease, its early stages involve the breakdown and loss of GAG and collagen from the extracellular matrix. There are other MRI-based methods targeting macromolecules as biomarkers of OA disease progression besides $T1_\rho$ MRI. Chemical Exchange Saturation Transfer (CEST) MRI is sensitive to proton exchange between –OH groups in GAG and water and hence highly specific to GAG content. The feasibility of CEST MRI to detect GAG *in vivo* (gagCEST) was recently demonstrated in cartilage of the knee joint by experiments on 7T* whole-body Siemens MRI scanners [36]. This study also demonstrated that gagCEST values obtained from images without correcting for B_0 inhomogeneity (0.6 ppm) could lead to some inaccuracy of the final quantifications [37]. $T1_\rho$ MRI has already been applied to clinical research by several groups and was shown to be a promise method in evaluating early OA by demonstrating its sensitivity and specificity to cartilage physiology and biochemistry as well as its ability to detect progression of the disease. Larger multi-center studies will be required to develop standard protocols in order for these methods to be translated to clinical practice.

Acknowledgements

This work was performed at a Biomedical Technology Research Center supported by NCRR (P41 RR002305) and NIBIB (P41 EB015893) and grants R01AR45404, R01AR051041 from NIAMS.

*The 7T system is an investigational device. Limited by U.S. federal law to investigational use. The product is still under development and not commercially available yet. Its future availability cannot be ensured.

References

1 Brandt KD, Doherty M, Lohmander S. Osteoarthritis. Oxford ; New York: Oxford University Press; 2003. xii, 511 p. p.

2 Ogston A. The biological functions of the glycosaminoglycans. In: Balazs E, editor. Chemistry and Molecular Biology of the Intercellular Matrix. Volume 3. New York: Academic Press; 1970. p 1231–1240.

3 Maroudas AI. Balance between swelling pressure and collagen tension in normal and degenerate cartilage. Nature 1976;260(5554):808-809.

4 Maroudas A. Physicochemical properties of articular cartilage. In: Freeman MAR, editor. Adult articular cartilage. 2nd ed. Kent, England: Pitman Medical; 1979. p 215-290.

5 Glasson SS, Askew R, Sheppard B, Carito B, Blanchet T, Ma HL, Flannery CR, Peluso D, Kanki K, Yang Z, Majumdar MK, Morris EA. Deletion of active ADAMTS5 prevents cartilage degradation in a murine model of osteoarthritis. Nature 2005;434(7033):644-648.

6 Stanton H, Rogerson FM, East CJ, Golub SB, Lawlor KE, Meeker CT, Little CB, Last K, Farmer PJ, Campbell IK, Fourie AM, Fosang AJ. ADAMTS5 is the major aggrecanase in mouse cartilage *in vivo* and in vitro. Nature 2005;434(7033):648-652.

7 Bellamy N, Buchanan WW, Goldsmith CH, Campbell J, Stitt LW. Validation study of WOMAC: a health status instrument for measuring clinically important patient relevant outcomes to antirheumatic drug therapy in patients with osteoarthritis of the hip or knee. J Rheumatol 1988;15(12):1833-1840.

8 Roos EM, Roos HP, Lohmander LS, Ekdahl C, Beynnon BD. Knee Injury and Osteoarthritis Outcome Score (KOOS)--development of a self-administered outcome measure. J Orthop Sports Phys Ther 1998;28(2):88-96.

9 Blackburn WD, Jr., Chivers S, Bernreuter W. Cartilage imaging in osteoarthritis. Seminars in Arthritis & Rheumatism 1996;25(4):273-281.

10 Heron CW. Review article: MRI of the knee. British Journal of Radiology 1993;66(784):292-302.

11 Potter HG, Linklater JM, Allen AA, Hannafin JA, Haas SB. Magnetic resonance imaging of articular cartilage in the knee - An evaluation with use of fast-spin-echo imaging. Journal of Bone and Joint Surgery 1998;80A(9):1276-1284.

12 Recht M, Bobic V, Burstein D, Disler D, Gold G, Gray M, Kramer J, Lang P, McCauley T, Winalski C. Magnetic resonance imaging of articular cartilage. Clin Orthop 2001(391 Suppl):S379-396.

13 Zhang W, Moskowitz RW, Nuki G, Abramson S, Altman RD, Arden N, Bierma-Zeinstra S, Brandt KD, Croft P, Doherty M, Dougados M, Hochberg M, Hunter DJ, Kwoh K, Lohmander LS, Tugwell P. OARSI recommendations for the management of hip and knee osteoarthritis, Part II: OARSI evidence-based, expert consensus guidelines. Osteoarthritis Cartilage 2008;16(2):137-162.

14 Dijkgraaf LC, de Bont LG, Boering G, Liem RS. The structure, biochemistry, and metabolism of osteoarthritic cartilage: a review of the literature. J Oral Maxillofac Surg 1995;53(10):1182-1192.

15 Borthakur A, Mellon E, Niyogi S, Witschey W, Kneeland J, Reddy R. Sodium and T1rho MRI for molecular and diagnostic imaging of articular cartilage. NMR Biomed 2006;19(7):781-821.

16 Duvvuri U, Goldberg AD, Kranz JK, Hoang L, Reddy R, Wehrli FW, Wand AJ, Englander SW, Leigh JS. Water magnetic relaxation dispersion in biological systems: The contribution of proton exchange and implications for the noninvasive detection of cartilage degradation. Proc Natl Acad Sci U S A 2001;98(22):12479-12484.

17 Santyr GE, Henkelman RM, Bronskill MJ. Spin locking for magnetic resonance imaging with application to human breast. Magn Reson Med 1989;12(1):25-37.

18 Lamminen AE, Tanttu JI, Sepponen RE, Pihko H, Korhola OA. T1rho dispersion imaging of diseased muscle tissue. Br J Radiol 1993;66(789):783-787.

19 Dixon WT, Oshinski JN, Trudeau JD, Arnold BC, Pettigrew RI. Myocardial suppression *in vivo* by spin locking with composite pulses. Magn Reson Med 1996;36(1):90-94.

20 Charagundla SR, Stolpen AH, Leigh JS, Reddy R. Off-resonance proton T1r dispersion imaging of 17O-enriched tissue phantoms. Magn Reson Med 1998;39(4):588-595.

21 Mlynarik V, Trattnig S, Huber M, Zembsch A, Imhof H. The role of relaxation times in monitoring proteoglycan depletion in articular cartilage. J Magn Reson Imaging 1999;10(4):497-502.

22 Grohn OHJ, Kettunen MI, Makela HI, Penttonen M, Pitkanen A, Lukkarinen JA, Kauppinen RA. Early detection of irreversible cerebral ischemia in the rat using dispersion of the magnetic resonance imaging relaxation time, T1rho. J Cereb Blood Flow Metab 2000;20(10):1457-1466.

23 Poptani H, Duvvuri U, Miller CG, Mancuso A, Charagundla S, Fraser NW, Glickson JD, Leigh JS, Reddy R. T1rho imaging of murine brain tumors at 4 T. Acad Radiol 2001;8(1):42-47.

24 Duvvuri U, Poptani H, Feldman M, Nadal-Desbarats L, Gee MS, Lee WM, Reddy R, Leigh JS, Glickson JD. Quantitative T(1rho) magnetic resonance imaging of RIF-1 tumors *in vivo*: detection of early response to cyclophosphamide therapy. Cancer Research 2001;61(21):7747-7753.

25 Borthakur A, Wheaton A, Gougoutas A, Akella S, Regatte R, Charagundla S, Reddy R. *In vivo* measurement of T1rho dispersion in the human brain at 1.5 tesla. J Magn Reson Imaging 2004;19(4):403-409.

26 Wheaton A, Dodge G, Borthakur A, Kneeland J, Schumacher H, Reddy R. Detection of changes in articular cartilage proteoglycan by T(1rho) magnetic resonance imaging. J Orthop Res 2005;23(1):102-108.

27 Li X, Han ET, Ma CB, Link TM, Newitt DC, Majumdar S. *In vivo* 3T spiral imaging based multi-slice T(1rho) mapping of knee cartilage in osteoarthritis. Magn Reson Med 2005;54(4):929-936.

28 Xia Y, Farquhar T, Burton-Wurster N, Lust G. Origin of cartilage laminae in MRI. Journal of Magnetic Resonance Imaging 1997;7(5):887-894.

29 Akella S, Regatte R, Wheaton A, Borthakur A, Reddy R. Reduction of residual dipolar interaction in cartilage by spin-lock technique. Magn Reson Med 2004;52(5):1103-1109.

30 Majumdar S, Li X, Blumenkrantz G, Saldanha K, Ma CB, Kim H, Lozano J, Link T. MR imaging and early cartilage degeneration and strategies for monitoring regeneration. J Musculoskelet Neuronal Interact 2006;6(4):382-384.

31 Lozano J, Saadat E, Li X, Majumdar S, Ma CB. Magnetic resonance T(1 rho) imaging of osteoarthritis: a rabbit ACL transection model. Magn Reson Imaging 2009;27(5):611-616.

32 Bolbos RI, Link TM, Ma CB, Majumdar S, Li X. T1rho relaxation time of the meniscus and its relationship with T1rho of adjacent cartilage in knees with acute ACL injuries at 3 T. Osteoarthritis Cartilage 2009;17(1):12-18.

33 Witschey W, Borthakur A, Fenty M, Kneeland B, Lonner J, McArdle E, Sochor M, Reddy R. T1rho MRI quantification of arthroscopically confirmed cartilage degeneration. Magn Reson Med 2010;63(5):1376-1382.

34 de Beer JF, Bhatia DN, van Rooyen KS, Du Toit DF. Arthroscopic debridement and biological resurfacing of the glenoid in glenohumeral arthritis. Knee Surg Sports Traumatol Arthrosc 2010;18(12):1767-1773.

35 McNickle AG, L'Heureux DR, Provencher MT, Romeo AA, Cole BJ. Postsurgical glenohumeral arthritis in young adults. Am J Sports Med 2009;37(9):1784-1791.

36 Singh A, Haris M, Cai K, Kassey VB, Kogan F, Reddy D, Hariharan H, Reddy R. Chemical exchange saturation transfer magnetic resonance imaging of human knee cartilage at 3 T and 7 T. Magn Reson Med 2012;68(2):588-594.

37 Ling W, Regatte R, Navon G, Jerschow A. Assessment of glycosaminoglycan concentration *in vivo* by chemical exchange-dependent saturation transfer (gagCEST). Proc Natl Acad Sci U S A 2008;105(7):2266-2270.

38 Witschey W, Borthakur A, Elliott M, Fenty M, Sochor M, Wang C, Reddy R. T1rho-prepared balanced gradient echo for rapid 3D T1rho MRI. J Magn Reson Imaging 2008;28(3):744-754.

Contact
Ari Borthakur, Ph.D.
Associate Director
Center for Magnetic Resonance & Optical Imaging
Perelman School of Medicine
at the University of Pennsylvania
B1 Stellar-Chance Laboratories
422 Curie Boulevard
Philadelphia, PA 19104-6100
USA
Phone: +1 (215) 573-8482
Fax: +1 (215) 573-2113
borthaku@upenn.edu
Web: http://med.cmroi.upenn.edu